Geol. Mag. **149** (*2*), *2012, pp. 208–220. © Cambridge University Press 2011*
doi:10.1017/S0016756811000653

Jurassic to Early Cretaceous postaccretional sinistral transpression in north-central Chile (latitudes 31–32° S)

UWE RING*†, ARNE P. WILLNER‡, PAUL W. LAYER§ & PETER P. RICHTER¶

*Department of Geological Sciences, Canterbury University, Christchurch 8140, New Zealand
‡Institut für Geologie, Mineralogie & Geophysik, Ruhr-Universität, D-44780 Bochum, Germany
§Department of Geology & Geophysics, University of Alaska, Fairbanks, USA
¶Institut für Geologie, Christian-Albrechts Universität, 24118 Kiel, Germany

(*Received* 30 May 2010; *accepted* 9 February 2011; *first published online* 16 August 2011)

Abstract – We describe the geometry and kinematics of a Jurassic to Early Cretaceous transpressive sinistral strike-slip system within a metamorphic basement inlier of the Mesozoic magmatic arc near Bahia Agua Dulce at latitudes 31–32° S in north-central Chile and discuss possible relations with the Atacama Fault System further north. Sinistral transpression overprints structures of an accretionary system that is represented by the metamorphic basement. Sub-vertical semi-ductile NNW-striking strike-slip shear zones are the most conspicuous structures. Chlorite and sericite grew, and white mica and quartz dynamically recrystallized, suggesting low-grade metamorphic conditions during semi-ductile deformation. Folds at the 10–100 metre scale developed before and during strike-slip shearing. The folds are deforming a former sub-horizontal transposition foliation that originated during prior accretion processes. The folds have axes sub-parallel to the strike-slip shear zones and sub-vertical axial surfaces indicating a component of shortening parallel to the shear-zone boundaries, suggesting an overall transpressive deformation regime. Transpressive strike-slip deformation also affects Middle Triassic (Anisian) basal breccias of the El Quereo Formation. ^{40}Ar–^{39}Ar laser ablation ages of synkinematically recrystallized white mica in one of the shear zones provide an age of 174–165 Ma for the waning stages of semi-ductile strike-slip shearing. The semi-ductile shear zones are cut by mafic and rhyolite dykes. Two rhyolite dykes yield ^{40}Ar–^{39}Ar ages of 160.5 ± 1.7 Ma and 131.9 ± 1.7 Ma, respectively. The latter dyke has been affected by brittle faulting. Fault-slip analysis shows that the kinematics of the faulting event is similar to the one of the semi-ductile shearing event, suggesting that sinistral transpression continued after ∼130 Ma. Timing, kinematics and geographic position suggest that the shear zones at Bahia Agua Dulce represent a southern continuation of the prominent Atacama Fault System that affected the Jurassic/Early Cretaceous arc over its ∼1400 km length.

Keywords: folds, shear zones, transpression, ^{40}Ar–^{39}Ar dating, South America, Chile, Atacama Fault System.

1. Introduction

The crust of the Coastal Cordillera of Chile between 30° and 55° S is dominated by metamorphic basement rocks that represent a continuous chain of deep-seated accretionary systems of Permo-Carboniferous age in the north and Mesozoic age in the south (Hervé, 1988; Hervé *et al*. 2007; Willner *et al*. 2011: this issue). The fundamental architecture of the accretionary system was first shown at an undisturbed section at about 35° S (Rio Maule east of Constitución) by Richter *et al*. (2007): a belt of frontally accreted metagreywacke in upper levels of the accretion system (Eastern Series) continuously grades with increasing deformation into basally accreted deeper levels consisting of transposed metagreywacke series with intercalated metabasite of oceanic origin (Western Series). This change in the mode of accretion reflects adjustments in the flow field during accretion (cf. Feehan & Brandon, 1999; Ring & Brandon, 1999; Ring, Brandon & Ramthun, 2001; Ring, Mortimer & Deckert, unpub. report, in prep.: Critical wedge theory explains large-scale tectonic evolution of the Cretaceous Torlesse accretionary wedge and associated magmatic arc, New Zealand). Frontal accretion of the Eastern Series gave rise to sub-horizontal shortening in a thickening flow field that was superseded by basal accretion of the Western Series causing sub-vertical shortening in a thinning flow field (Richter *et al*. 2007).

In many places along the Coastal Cordillera the accretionary complex has been variably overprinted by later structures. One such area is exposed at Bahia Agua Dulce (31–32° S) in north-central Chile (Figs 1, 2). In the Bahia Agua Dulce area, the once coherent architecture of the late Palaeozoic fore-arc system is overprinted by numerous steep semi-ductile to cataclastic strike-slip shear zones, which modified the accretional architecture (Rebolledo & Charrier, 1994). At 34–35° S, Willner, Richter & Ring (2009) showed that steep semi-ductile to cataclastic strike-slip shear zones have sinistral kinematics and are probably Jurassic in age.

†Author for correspondence: uwe.ring@canterbury.ac.nz

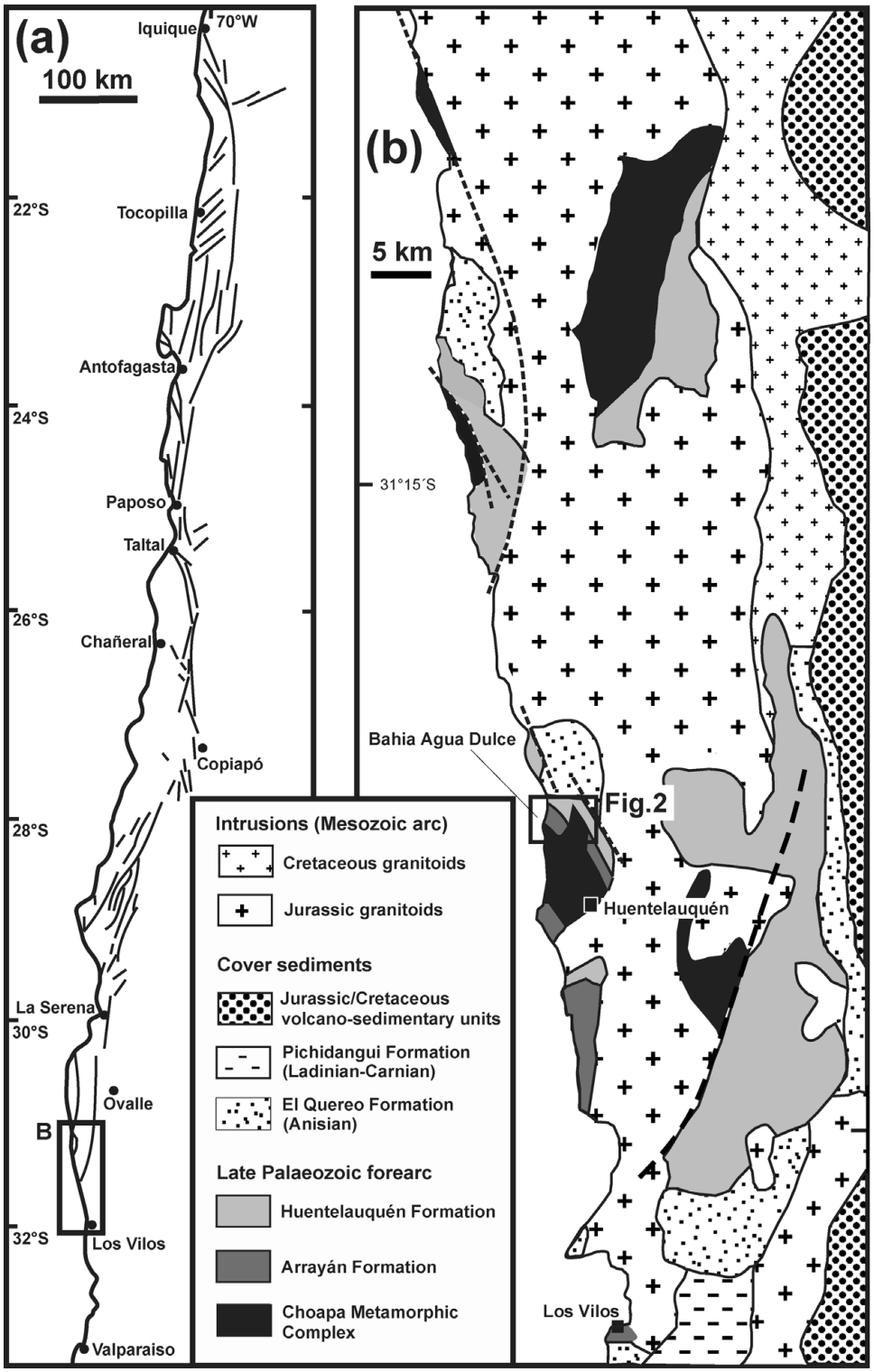

Figure 1. (a) Schematic tectonic map of northern and central Chile showing faults related to the Atacama Fault System (after Charrier, Pinto & Rodríguez, 2008). (b) Geological map of the Chilean coastal range at 31–32° S (based on Rivano & Sepúlveda, 1983 and Rebelledo & Charrier, 1994). Note that the Jurassic to Early Cretaceous magmatic arc has moved into the late Palaeozoic and Triassic accretionary wedge. Location of Figure 2 at Bahia Agua Dulce is shown.

The conspicuous postaccretional structures at 31–32° S and 34–35° S resemble those of the Jurassic–Early Cretaceous Atacama Fault System that dominates the Jurassic–Early Cretaceous magmatic arc over most of its length of ∼1400 km (Charrier, Pinto & Rodríguez, 2008 and references therein) (Fig. 1a). The geometry, kinematics and timing of deformation of the Atacama Fault System are known at the regional-scale in northern Chile (Scheuber & Andriessen, 1990; Grocott *et al*. 1994; Scheuber & Gonzalez, 1999; Grocott & Taylor, 2002). Deformation in the Atacama Fault System mainly involves sinistral

https://doi.org/10.1017/S0016756811000653 Published online by Cambridge University Press

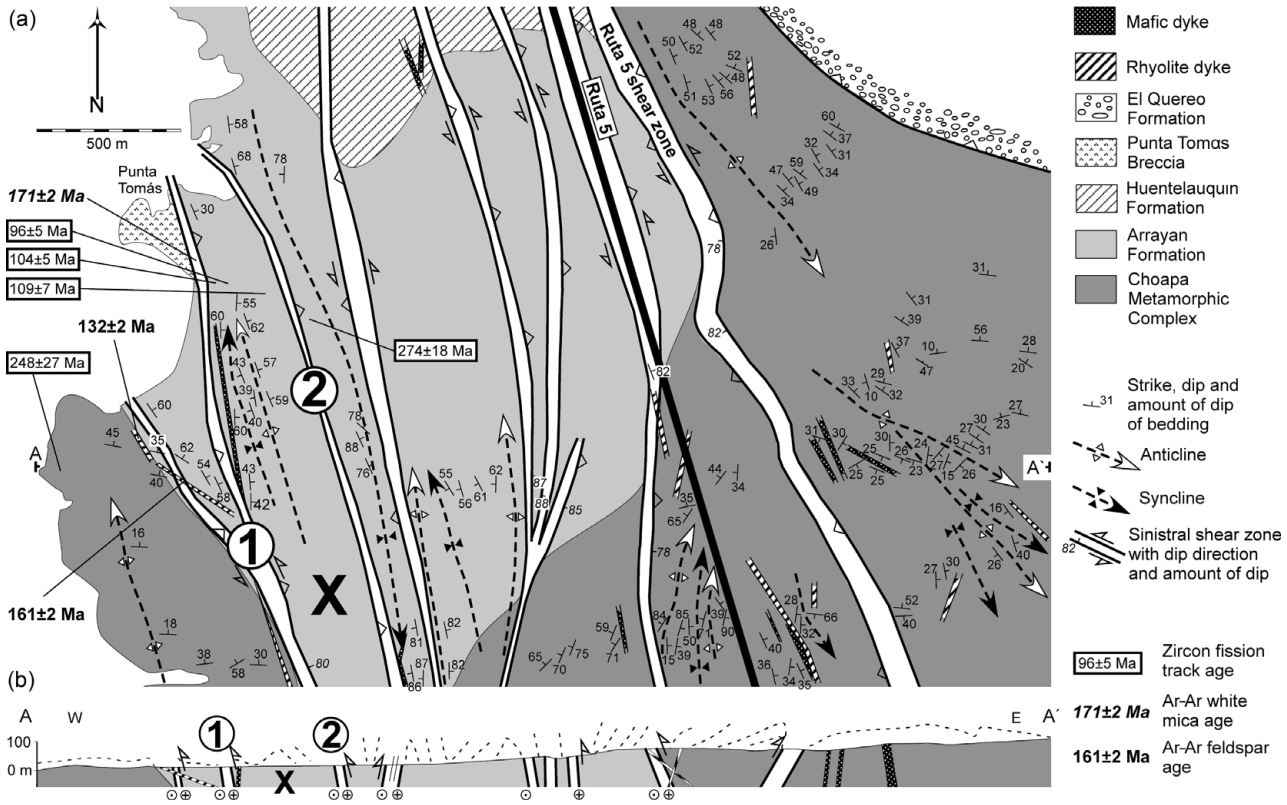

Figure 2. Geological-tectonic map (a) and E–W cross-section (b) of the Bahia Agua Dulce area (based on map of Rebelledo & Charrier, 1994 and own mapping; refer to Fig. 1 for location of map). The map shows the major sinistral strike-slip faults and also the large-scale F3 folds that affect the entire fore-arc sequence. Also shown are mafic and rhyolitic dykes, which cross-cut the shear zones and the F3 folds. Note that it is conceivable that the Arrayán Formation represents a huge N-plunging synclinal core between the E-dipping shear zone 1 at the coast and the W-dipping 'Ruta 5' shear zone inland. Also shown are five zircon fission-track ages (X marks a block with anomalously young zircon fission-track ages of ∼100 Ma) and the ^{40}Ar–^{39}Ar age obtained from synkinematically recrystallized white mica from the shear zone that separates the metamorphic basement from the Triassic Punta Tomás Breccia (Willner *et al*. 2011). Also shown are ^{40}Ar feldspar ages of samples CH02-78 (161 ± 2 Ma) and CH02-77 (132 ± 2 Ma).

transpressional movement from about 195 to 125 Ma. In its northern part, sinistral transpression across the Atacama Fault System commenced under granulite- to amphibolite-facies conditions within the magmatic arc. Subsequently greenschist-facies shear zones showing sinistral strike-slip and thrust kinematics resulting from NW-directed horizontal shortening formed in a fore-arc setting. Scheuber & Gonzalez (1999) argued that there was a short period of extensional deformation across the Atacama Fault System between ∼160–145 Ma involving arc-normal extension accompanied and followed by the intrusion of two generations of dykes, the first of which strikes NE and the younger one striking NW.

The aim of this paper is to describe the geometry and kinematics of the prominent steep shear zones that overprinted the late Palaeozoic accretionary complex at 31–32° S. We will also present age data constraining the timing of shear-zone activity and discuss the possible relation of the shear zones to the regional large-scale structures of the Atacama Fault System. A companion paper (Willner *et al*. 2011) presents ^{40}Ar–^{39}Ar and zircon fission-track (ZFT) ages as well as *P–T* data constraining aspects of the accretionary history and its subsequent overprint at 31–32° S.

2. Setting

In the Coastal Cordillera of central Chile the Eastern and Western Series are traditionally distinguished within the pre-Andean coastal accretionary belt (Aguirre, Hervé & Godoy, 1972; Hervé, 1988; Willner *et al*. 2005) as units of contrasting tectonic setting. Throughout central Chile, the Eastern Series structurally overlies the Western Series (E. Godoy, unpub. B.Sc. thesis, Univ. Chile, Santiago, 1970; Richter *et al*. 2007). The overlying Eastern Series first formed by frontal accretion to this accretionary wedge, and the underlying Western Series subsequently by basal accretion to the base of a late Palaeozoic to Triassic subduction complex (Hervé, 1988; Willner *et al*. 2005; Glodny *et al*. 2005; Richter *et al*. 2007). Both series consist dominantly of metagreywacke and metapelite, interpreted as continent-derived, turbidite successions (Hervé, 1988). Oceanic crust-derived rocks such as metachert, metabasite and serpentinite are largely absent in the Eastern Series, but typically occur as intercalations within the Western Series.

The crust of the coastal range from 20–30° S is dominated by rocks of the prominent Jurassic–Early Cretaceous magmatic arc, and the metamorphic

https://doi.org/10.1017/S0016756811000653 Published online by Cambridge University Press

basement (the term metamorphic basement relates to all metamorphosed rocks in Chile) forms isolated inliers within this arc. At Bahia Agua Dulce, the upper levels of the accretionary system are not overprinted by a high-temperature/low-pressure metamorphism as in many regions throughout central Chile and are unconformably overlain by retrowedge shelf deposits (Thiele & Hervé, 1984; Rebelledo & Charrier, 1994).

The metamorphic basement in north-central Chile at 31–32° S shows various levels of a fore-arc system including an accretionary wedge that is strongly overprinted by Mesozoic tectonic processes. Four units are usually distinguished (Rivano & Sepúlveda, 1983, 1985; Thiele & Hervé, 1984; Rebelledo & Charrier, 1994):

(1) The Choapa Metamorphic Complex represents the structurally lowermost unit of the fore-arc system and comprises low-grade rocks (metagreywacke, greenschist) that are pervasively deformed by an originally sub-horizontal transposition foliation. The Choapa Metamorphic Complex can be correlated with the Western Series south of 34° S owing to similarities of lithology, structures, metamorphic grade and maximum depositional age (Willner *et al*. 2008).

(2) The Arrayán Formation is dominated by very low-grade monotonous metagreywacke of turbiditic origin and correlates with the Eastern Series (Willner *et al*. 2008). The Arrayán Formation shows similar structures to the frontally accreted Eastern Series south of 34° S (Richter *et al*. 2007) such as chevron folds of bedding planes. A Late Devonian to Early Carboniferous biostratigraphical age is assigned to the Arrayán Formation (Rebelledo & Charrier, 1997). Dating the youngest detrital magmatic zircon with the U–Pb system, Willner *et al*. (2008) derived a maximum depositional age of 343 Ma for the Arrayán Formation. This is significantly older than the maximum depositional age of the Choapa Metamorphic Complex, suggesting that basal accretion followed frontal accretion in time in Chile, as has first been shown south of latitude 34° S by Richter *et al*. (2007). Following Willner *et al*. (2008), we also include the Agua Dulce metaturbidites of Rebelledo & Charrier (1997) in the Arrayán Formation because of a similar maximum depositional age of 337 Ma. The Agua Dulce metaturbidites constitute the more strongly deformed structural base of the Arrayán Formation.

(3) The Huentelauquén Formation unconformably overlies the Arrayán Formation (Rebelledo & Charrier, 1997). It is a heterogeneous sedimentary sequence of shelf deposits comprising metasandstone with slate and metaconglomerate intercalations at the base overlain by thick polymict metaconglomerate, platform limestone and metasandstone. Rivano & Sepúlveda (1983, 1985) assign a Late Carboniferous to Permian biostratigraphic age to the Huentelauquén Formation. U–Pb dating of detrital zircon in pebbles of the metaconglomerate demonstrates a maximum age of deposition of 303 Ma for the Huentelauquén Formation. Therefore, Willner *et al*. (2008) concluded that deposition of the Huentelauquén Formation was concomitant with that of the Choapa Metamorphic Complex. The Huentelauquén Formation was deposited in a retrowedge position as already inferred by Thiele & Hervé (1984).

(4) The non-metamorphic El Quereo Formation regionally overlies the rocks of the fore-arc system unconformably with a prominent breccia (Punta Tomás Breccia) at its base. In our study area, the contacts of the El Quereo Formation with the accretionary wedge rocks are tectonic. The El Quereo Formation consists of fine- to coarse-grained sandstones with pelitic and conglomeratic intercalations. It has an Anisian (245–237 Ma) biostratigraphic age (Cecioni & Westermann, 1968). However, the non-fossiliferous Punta Tomás Breccia at the base may be somewhat older.

Rb–Sr whole-rock isochron ages of 220 ± 20 Ma for a gabbro and 200 ± 10 Ma for a monzogranite are interpreted as intrusion ages during lithospheric extension at 31–32° S (Irwin *et al*. 1988). This magmatic event is concomitant with basin formation in central Chile related to the deposition of the El Quereo Formation (Charrier, Pinto & Rodríguez, 2008). Mafic and rhyolitic dykes intruded the entire sequence from Late Triassic to Early Cretaceous times. K–Ar ages of hornblende in mafic dykes yielded a huge spread in ages from 213–133 Ma (Irwin *et al*. 1988). During Jurassic to Early Cretaceous times, a prominent N–S-trending magmatic arc developed along the entire coast between 21° and 34° S (Parada *et al*. 2007). At 28° S to 32° S the metamorphic basement forms large inliers within this arc. In Mid Cretaceous times a prominent phase of E–W shortening affected the region at about 32° S (Arancibia, 2004).

3. Architecture of the Bahia Agua Dulce area

To better understand the kinematics of the prominent sinistral strike-slip shear zones, we mapped a ∼9 km^2 area near Bahia Agua Dulce north of Los Vilos in detail (Fig. 2). Rebolledo & Charrier (1994) and Rebolledo, Solari & Contreras (2003) already described the deformation history of the fore-arc sequence in this area and showed the extent of the sinistral strike-slip shear zones.

The structurally deepest unit is the Choapa Metamorphic Complex in the southwestern corner of the Bahia Agua Dulce area and in the eastern half of the study area (Fig. 2). The Arrayán Formation and the Huentelauquén Formation rest above the Choapa Metamorphic Complex. However, this normal succession is significantly disturbed by the 'Ruta 5' shear zone and shear zones to the west of the 'Ruta 5' shear zone, which bring the Choapa Metamorphic Complex above the Arrayán Formation and the Huentelauquén Formation (Fig. 2). The Arrayán Formation rests along a sinistral reverse fault above the Punta Tomás Breccia at the coast. The El Quereo Formation occurs unconformably above the Choapa Metamorphic Complex in the northeastern corner of the study area.

https://doi.org/10.1017/S0016756811000653 Published online by Cambridge University Press

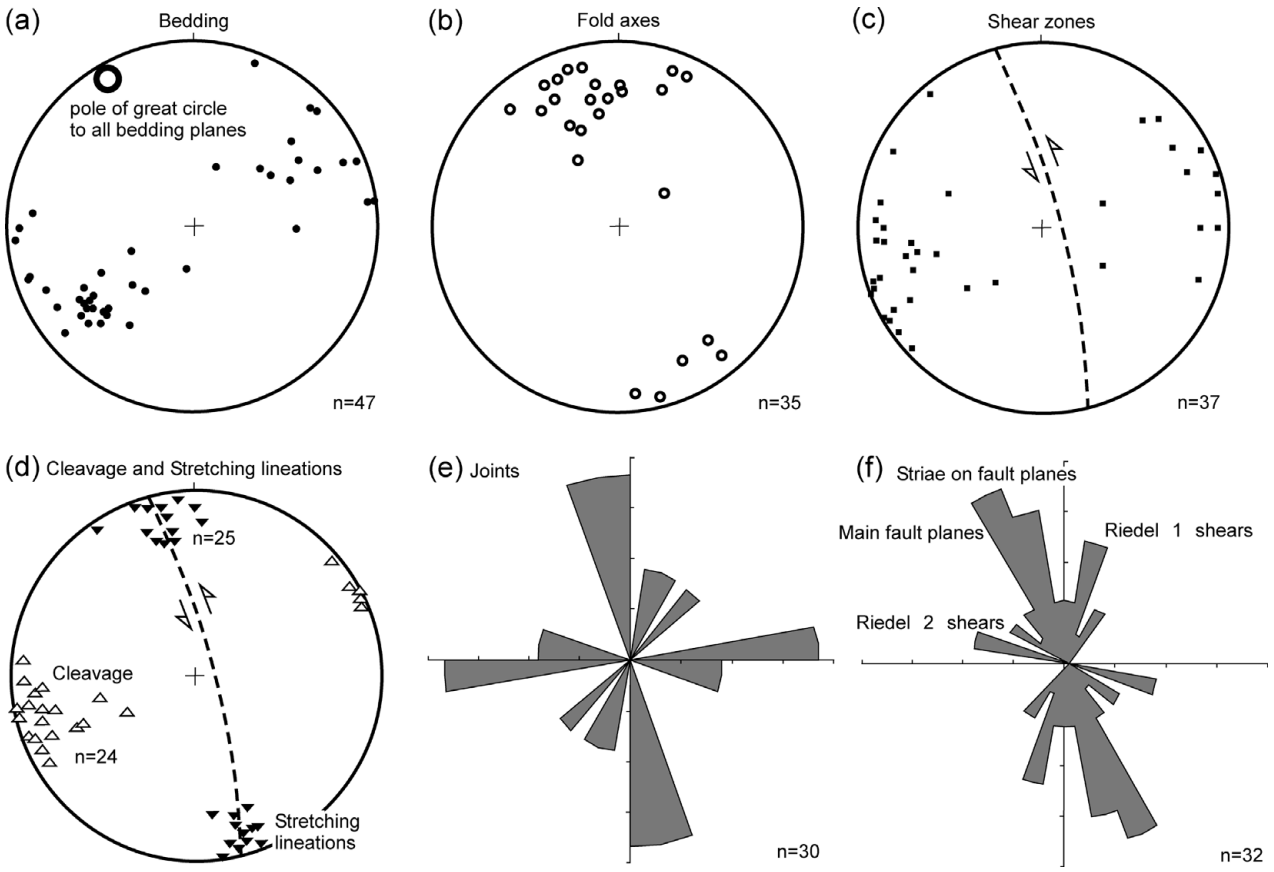

Figure 3. (a–d) Stereographic projections. (a) Poles to bedding in the Arrayán and Huentelauquén formations (note that average pole to bedding coincides with F3 fold axes shown in (b)). (b) F3 fold axes. (c) Poles to shear zones (dashed great circle shows average trace of all shear zones combined). (d) Cleavage and stretching lineations associated with the strike-slip shear zones (dashed great circle as in (c)). (e) Rose diagram of joint surfaces in the Arrayán and Huentelauquén formations. (f) Rose diagram of striations on major shear planes and on Riedel 1 (synthetic, i.e. sinistral) and Riedel 2 (antithetic, i.e. dextral) shear planes.

The overall structure of the Bahia Agua Dulce area is dominated by the NNW-striking sub-vertical shear zones, which cut across the contacts between the Choapa Metamorphic Complex, the Arrayán Formation and the Huentelauquén Formation. The shear zones mainly dip steeply to the east, with the easternmost 'Ruta 5' shear zone being the most prominent in the study area and dipping steeply west (Fig. 2).

The shear zones are associated with folds at the 10–100 metre scale. The folds have axes sub-parallel to the strike-slip shear zones and have sub-vertical axial surfaces and sub-horizontal fold axes and affect all mapped units in Figure 2. Steeply dipping mafic and rhyolite dykes cut both the shear zones and the associated folds.

It is feasible that the occurrence of the Arrayán Formation represents a huge synclinal transpressional core bounded by the E-dipping shear zone at the coast (shear zone 1 in Fig. 2) and the W-dipping 'Ruta 5' shear zone in the east.

4. Deformation

4.a. Pre-shear-zone deformation

The rocks of the Choapa Metamorphic Complex, and the Arrayán and Huentelauquén formations show the deformation structures typical for the Western and Eastern series elsewhere in central Chile. In the Arrayán and Huentelauquén formations, upright folds of bedding have a weakly developed axial-plane S1 foliation particularly bound to pelitic intercalations. In the Choapa Metamorphic Complex, S1 is folded about F2 folds, which are associated with an S2 axial-plane foliation. In most places S2 has almost totally obliterated S1 and is the penetrative foliation. Where S2 is sub-horizontal, F2 is isoclinal with highly attenuated limbs.

4.b. F3 folds and sub-vertical shear zones

The sub-vertical shear zones are the most conspicuous structures in the Bahia Agua Dulce area and the focus of this study. The dominant mechanical anisotropy in the various rock units, i.e. bedding in the Arrayán, Huentelauquén and El Quereo formations (Fig. 3a) and the S2 foliation in the Choapa Metamorphic Complex, is deformed into open to tight folds at the 10–100 metre scale. The axes of these F3 folds are sub-horizontal and trend NNE (Fig. 3b). The F3 folds are slightly asymmetric and the vergence is mainly to the west.

In the steeper western limb of the F3 folds sub-vertical semi-ductile shear zones formed (Fig. 3c). In

https://doi.org/10.1017/S0016756811000653 Published online by Cambridge University Press

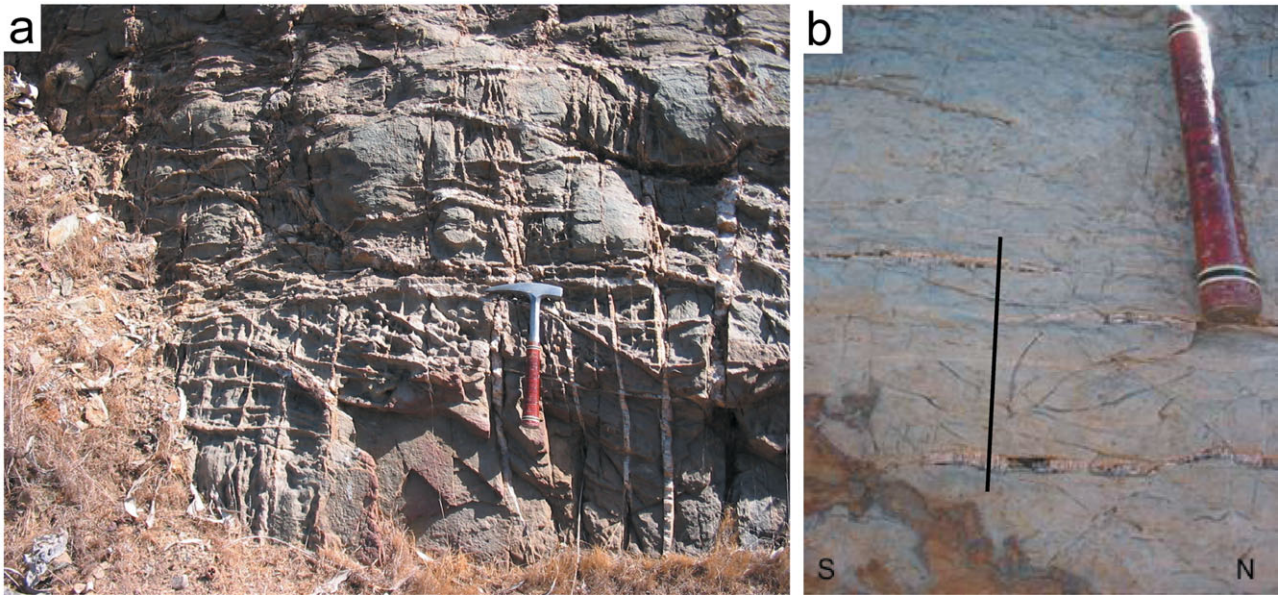

Figure 4. (Colour online) (a) Complex sets of extension veins in metapsammitic rocks of the Arrayán Formation. The youngest set of those veins is sub-horizontal and has sub-vertical fibres. (b) Close-up of outcrop shown in (a) highlighting vertical orientation of quartz fibres (indicated by solid line).

the Bahia Agua Dulce area the only exception is the 'Ruta 5' shear zone in the east, which developed on the eastern limb of a locally E-verging F3 fold. The sub-vertical shear zones range in thickness from a few centimetres to ~50 m. In the shear zones a penetrative sub-vertical foliation developed. In metapsammitic rock types quartz is dynamically recrystallized in quartz-rich foliation domains between thin phyllosilicate layers. Feldspar shows brittle microfaults forming local pull-apart structures into which fine-grained chlorite and sericite grew. Locally complex sets of extension veins formed in metapsammitic rocks of the Arrayán Formation in the vicinity of the shear zones (Fig. 4). The youngest set of those veins is sub-horizontal, has sub-vertical quartz fibres and appears to be associated with F3 folding and sub-vertical shearing. In mica-rich parts of the shear zones a continuous slaty cleavage developed and chlorite-filled shear bands formed in this cleavage. In these parts quartz is not recrystallized. On the cleavage planes a shallowly plunging stretching lineation is developed (Fig. 3d). About 75 % of the shear bands as well as the pull-apart structures in feldspar support a sinistral shear sense; the remaining ~25 % of the kinematic indicators yield a dextral shear sense.

During ongoing deformation in the sub-vertical shear zones, the semi-ductile shear-band structures were overprinted by discrete joints, shear fractures and fault planes (Fig. 3e, f). Three small-scale fault sets can be distinguished in the metamorphic basement (Fig. 3f).

(1) The majority of the faults formed sub-parallel to the shear zones. Most of these faults are sub-vertical and have sub-horizontal striations associated with them. The small-scale structures show sinistral offsets (Fig. 5a). However, some faults are dipping at angles between 40° and 70° and have more deeply plunging striations on them. These faults record oblique-reverse and reverse kinematics. (2) A minor fault set formed at angles of 20–30° to the shear zones. Small-scale kinematic indicators show that the kinematics of this minor fault set is the same as that of the major set, i.e. mainly sinistral (Riedel 1 shears in Fig. 3f). (3) A third set strikes almost perpendicular to the major fault set and is associated with dextral kinematic indicators (Riedel 2 shears in Fig. 3f). Overall, the pattern of small-scale faults is compatible with WNW-oriented shortening and NNE-directed extension associated with sinistral strike-slip deformation.

Strike-slip deformation also affects the Punta Tomás Breccia. Rebolledo, Solari & Contreras (2003) showed that a NNW-striking sinistral strike-slip fault cuts through the western part of the breccia at Bahia Agua Dulce. This fault is associated with a number of synthetic Riedel shears at angles of 25–35° to the main fault. We mapped striated fault planes associated with strike-slip faulting (Fig. 5b). The pattern of the small-scale faults is quite complicated. NNE-striking faults have reverse-slip kinematics and ~E-striking faults have normal-slip movement on them. Fault-slip analysis indicates that the kinematics of the striated planes is compatible with sinistral strike-slip faulting and similar to the fracture/striation pattern in the metamorphic basement (Fig. 5a).

The sinistral semi-ductile shear zones and faults are cut by mafic and rhyolite dykes (Fig. 6). Some of these dykes also have striated fault planes. Steeply dipping fault planes have striations and kinematic indicators showing sinistral strike-slip faulting. Rarely, reverse and oblique-reverse faulting has been observed. Faults at a high angle to the sinistral strike-slip faults have dextral oblique-normal kinematics.

https://doi.org/10.1017/S0016756811000653 Published online by Cambridge University Press

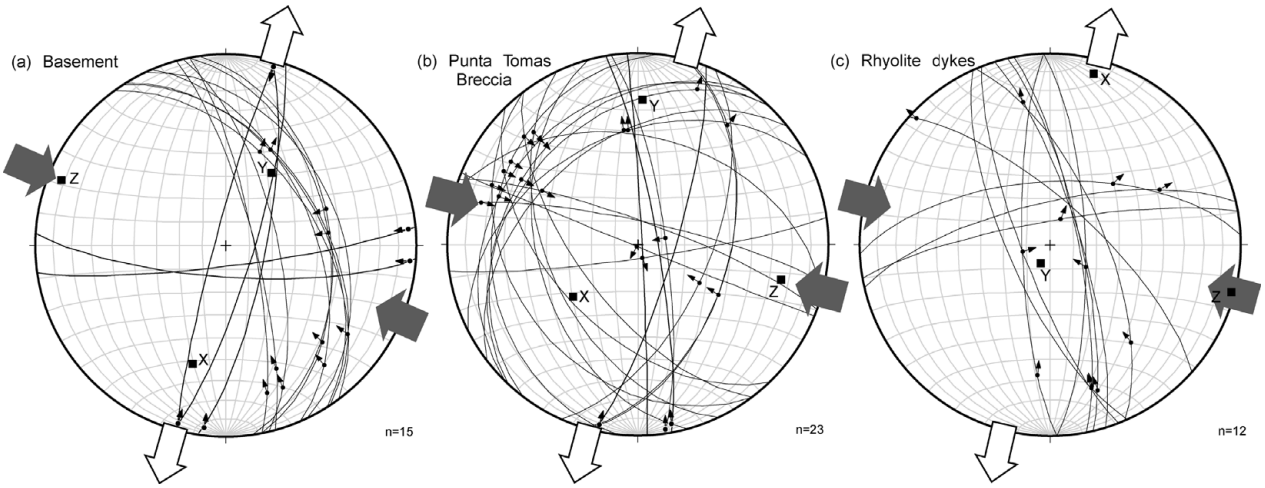

Figure 5. Fault-slip analysis using method of Marrett & Allmendinger (1990). The diagrams show great circles of fault planes and the projected trace of slickenside lineations in a lower-hemisphere equal-area projection. The deduced shortening (grey arrows) and extension (open arrows) directions from the fault patterns are indicated by arrows. (a) In the metamorphic basement rocks of the Choapa Metamorphic Complex and the Arrayán Formation, mainly ENE-dipping oblique-reverse faults have been mapped. In addition two near-vertical E–W-striking dextral strike-slip faults occur. (b) In the Triassic Punta Tomás Breccia the small-scale faults have more scattered attitudes with NW-dipping reverse faults apparently dominating. (c) In the rhyolite dykes, steeply dipping NNW-striking strike-slip and oblique-slip faults have been measured. Again E–W-striking dextral faults occur.

Figure 6. (Colour online) Steeply dipping rhyolite dyke cutting fabric in greywacke of Arrayán Formation.

Fault-slip analysis shows that the kinematics of the striated planes matches the kinematics as obtained from the metamorphic basement and the Punta Tomás Breccia recording sinistral strike-slip faulting (Fig. 5c). We dated two cross-cutting rhyolite dykes (see Section 5).

4.c. Tectonic interpretation of the F3 event

There appears to be an intimate relationship between F3 folds and the development of the NNW-striking sinistral shear zones, making it highly likely they formed during the same tectonic event. The folds record sub-horizontal maximum shortening and sub-vertical maximum extension, whereas the strike-slip shear zones indicate that maximum shortening and maximum extension had a sub-horizontal orientation. Overall, this suggests that the structures formed in a flattening strain field as a response to regional sinistral transpression. The flattening plane of this tectonic event would have been sub-vertical and sub-parallel to the present coastline. The coaxial flattening component of the general-shear deformation explains why about 25 % of the shear-sense indicators are dextral.

However, the stretching lineations are sub-horizontal and largely perpendicular to the ENE–WSW shortening direction inferred from the F3 folds. Given the transpressive character of the shear zone, the transport direction may have been steeper than the stretching lineations (Robin & Cruden, 1994; Glodny, Ring & Kühn, 2008).

The growth of chlorite and sericite and quartz recrystallization shows that sinistral transpression initiated under semi-ductile conditions. Semi-ductile shearing was succeeded by brittle deformation indicating regional cooling during sinistral transpression. We consider it likely that this cooling was chiefly caused by syntranspressional erosional exhumation of the rocks in Bahia Agua Dulce.

5. ^{40}Ar–^{39}Ar dating

5.a. Analytical procedures

^{40}Ar–^{39}Ar spot-analysis of white mica from micro-shear bands was done using laser ablation techniques described in Willner *et al*. (2011). ^{40}Ar–^{39}Ar analysis

https://doi.org/10.1017/S0016756811000653 Published online by Cambridge University Press

Table 1. Summary of ^{40}Ar–^{39}Ar step-heating analyses for feldspar

Grain size	Integrated age (Ma)	Plateau age (Ma)	Plateau information	Ca/K
CH02-78				
350–500 μm	160.0 ± 1.7	161.1 ± 1.7	4 fractions, 77% ^{39}Ar rel., MSWD = 0.8	0.6
>500 μm	157.1 ± 1.6	160.5 ± 1.7	4 fractions, 52% ^{39}Ar rel., MSWD = 2.1	0.3
CH02-77				
350–500 μm	126.7 ± 1.6	131.9 ± 1.7 (H)	4 fractions, 51% ^{39}Ar rel., MSWD = 0.3	21
Run #1		119.6 ± 2.2 (L)	4 fractions, 39% ^{39}Ar rel., MSWD = 0.3	
350–500 μm	124.0 ± 1.8	127.7 ± 2.6 (H)	6 fractions, 48% ^{39}Ar rel., MSWD = 0.2	20
Run #2		118.3 ± 2.3 (L)	3 fractions, 28% ^{39}Ar rel., MSWD = 1.0	
>500 μm	130.0 ± 2.5	135.4 ± 2.8 (H)	5 fractions, 53% ^{39}Ar rel., MSWD = 0.4	21
		122.1 ± 3.8 (L)	3 fractions, 24% ^{39}Ar rel., MSWD = 1.5	

Grain size – estimated range of minerals analysed based on sieve fraction designation. Integrated and plateau ages quoted at ±1σ. (H) – high closure temperature age, (L) – low closure temperature age (see Fig. 7). Note that some of the ages denoted as 'plateau' do not meet the criteria for 'true' plateaus (>50 % ^{39}Ar release), but are significant in preserving the age of a phase in the feldspar. Ca/K – total sample calcium to potassium ratio calculated from reactor produced ^{37}Ar and ^{39}Ar.

of feldspar from cross-cutting rhyolite dykes was performed at the University of Alaska Fairbanks, USA, and is described herein and in Layer (2000). The minerals separated from the samples were wrapped in aluminium foil and arranged in two levels, labelled top and bottom, within aluminium cans of 2.5 cm diameter and 4.5 cm height. Hornblende (MMhb1; Samson & Alexander, 1987) with an age of 513.9 Ma (Lanphere & Dalrymple, 2000) was included on each level with each set of unknowns to monitor the neutron flux. The samples were irradiated in position 5c of the uranium-enriched research reactor of McMaster University in Hamilton, Canada. Upon their return from the reactor, the samples and monitors were loaded into 2 mm diameter holes in a copper tray. The copper tray was then loaded in an ultra-high vacuum extraction line. The monitors were fused using a 6-watt argon-ion laser. Argon purification was achieved using a liquid nitrogen cold trap and a SAES Zr–Al getter at 400 °C. The samples were then analysed in a VG-3600 mass spectrometer at the Geophysical Institute of the University of Alaska using the single-crystal step-heating technique (York *et al*. 1981; Layer, Hall & York, 1987; Layer, 2000). The argon isotopes measured were corrected for system blank, mass discrimination, as well as calcium, potassium and chlorine interference reactions following procedures outlined in McDougall & Harrison (1999). The weighted mean of the results obtained from the monitor samples was used in the ensuing calculations for their corresponding set of samples. All ages were calculated using the constants of Steiger & Jäger (1977) and are quoted to the 1σ level. The results are summarized in Table 1, and a complete data list is given in the online Appendix at http://journals.cambridge.org/geo.

5.b. Data

Both the large (<500 μm) and smaller (350–500 μm) feldspar grain-size fractions of sample CH02-78 show basically the same result (Fig. 7a). Both have well defined nearly identical plateau ages with a weighted mean age at 160.5 ± 1.7 Ma (based on four fractions in each size fraction with 52 % and 77 % ^{39}Ar release). Diffusion loss modelling indicates very small amounts of argon loss (∼1 %) at 80–70 Ma. This possible 'event' is not well constrained. The Ca/K ratios (as determined from reactor produced ^{37}Ar from Ca and ^{39}Ar from K) of these samples (Table 1) are consistent with them being predominantly potassium feldspar. There is no evidence of older ages (i.e. Triassic) preserved in these samples. If they were originally older than 161 Ma, this record has been erased completely, and the 161 Ma age represents a complete resetting event. Based on the spectra alone, we conclude that the sample rapidly cooled through the closure temperature of potassium feldspar at 160.5 ± 1.7 Ma. The simplest explanation would be that this represents the intrusion age of the rhyolite dyke.

Feldspar from sample CH02-77 has a much more complex spectrum than that of CH02-78 (Fig. 7b). We ran two runs of the smaller (350–500 μm) and one of the larger (<500 μm) grain-size fractions to confirm the spectrum shape. All three spectra show basically the same age information. There are two 'plateaus', one with an age of ∼132 Ma (three-sample weighted average of 131.6 ± 1.8 Ma based on high-temperature plateau ages) and one with a weighted mean age at ∼119 Ma (three-sample weighted average of 119.4 ± 1.4 Ma based on the low-temperature release ages). The total sample Ca/K ratios are ∼20, significantly higher than CH02-78, indicative of a more calcium-rich feldspar phase. In looking at the different plateaus, the low-temperature steps are characterized by Ca/K ratios between 10 and 20, while the high-temperature steps have Ca/K ratios between 20 and 30 (see online Appendix at http://journals.cambridge.org/geo), implying that there may be two phases of feldspar represented in this sample.

As with most complex age spectra, there are multiple interpretations. We interpret the low-temperature age of 119 Ma to reflect the time of a thermal(?) resetting event, or perhaps secondary feldspar growth, given the lower Ca/K ratio of that phase. Although the exact

https://doi.org/10.1017/S0016756811000653 Published online by Cambridge University Press

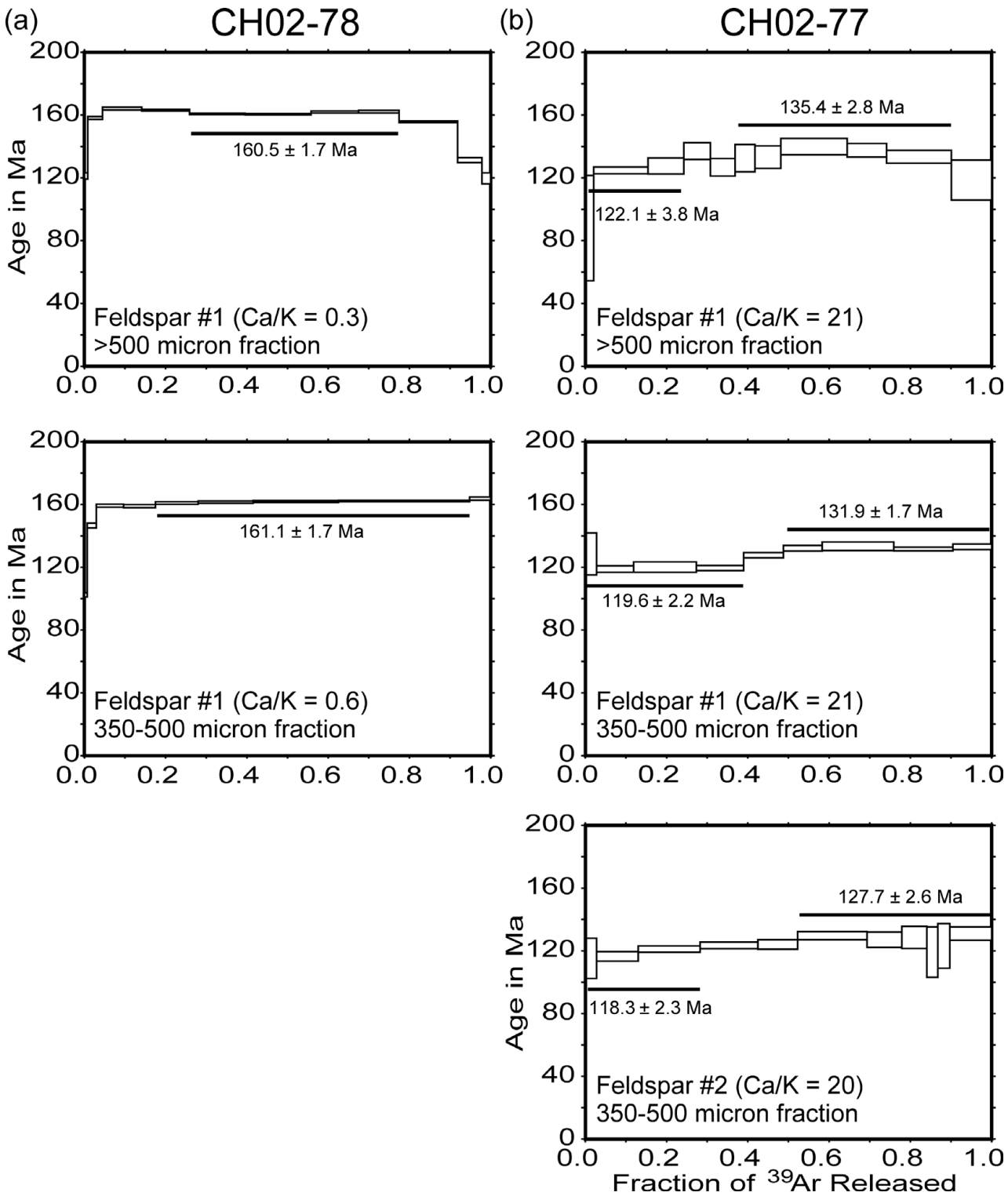

Figure 7. ^{40}Ar–^{39}Ar step-heating age spectra of feldspar from rhyolite veins. All ages are reported at the 1 sigma level.

age of the original cooling of this rhyolite is not well constrained, we tend to interpret the 132 Ma age as the age of intrusion of the rhyolite, and the younger age as reflecting some later 'event', perhaps associated with feldspar re-growth.

In a concomitant ^{40}Ar–^{39}Ar study of white mica in the Bahia Agua Dulce study area using laser ablation techniques (Willner *et al*. 2011), synkinematically grown fine-grained white mica was also dated in a metapsammite within a strike-slip shear zone at Punta Tomás. This rock (sample 06CH46) was strongly affected by the semi-ductile strike-slip shearing resulting in 0.1–1.0 mm thick micro-shear bands, where recrystallized white mica of < 10 μm size is enriched and also quartz dynamically recrystallized. Four spot ages from these zones resulted in similar ages at 164.8 ± 3.6 Ma, 173.0 ± 3.1 Ma, 169.7 ± 4.2 Ma and 173.7 ± 2.8 Ma (1σ errors). We interpret these ages as dating

https://doi.org/10.1017/S0016756811000653 Published online by Cambridge University Press

fluid-assisted dynamic recrystallization of white mica and thus the waning stages of the semi-ductile deformation event when fluid left the dated shear zone.

6. Discussion

6.a. Tectonic evolution at 31–32° S

The metamorphic basement succession made up by the Choapa Metamorphic Complex and the Arrayán and Huentelauquén formations shows a similar tectonic development as correlative metamorphic basement complexes along the coast of central Chile. The units were accreted to the South American margin in late Palaeozoic time and then were exhumed at rates of ~0.5 km Ma^{-1} in the latest Carboniferous and Early Permian (Willner *et al*. 2005). These rates are typical of subduction-related accretionary complexes along the North and South American Cordillera (Brandon & Vance, 1992; Ring & Brandon, 1994, 2008; Glodny *et al*. 2005; Ring, 2008; Bolhar & Ring, 2001). At Bahia Agua Dulce, parts of the metamorphic basement were at the surface by Middle Triassic time when the Punta Tomás Breccia at the base of the Anisian El Quereo Formation was deposited on them. Further east and south, the El Quereo Formation unconformably overlies the Arrayán and Huentelauquén formations.

The most prominent structures at Bahia Agua Dulce are the steep strike-slip shear zones that cut through the metamorphic basement and the Punta Tomás Breccia (Rebolledo & Charrier, 1994; Rebolledo, Solari & Contreras, 2003). The Punta Tomás Breccia contains strongly angular clasts indicating almost no transport and is interpreted to have been deposited during activity of extensional faults at the bottom of extensional escarpments in or slightly before the Anisian (Charrier, Pinto & Rodríguez, 2008). The brittle deformation structures in the breccia are compatible with very shallow level faulting. However, in large parts of the metamorphic basement the deformation structures indicate higher temperatures of around 300 °C (e.g. recrystallized quartz), suggesting that deformation occurred at depths of 10–15 km or more. The juxtaposition of rocks that experienced strike-slip deformation at different crustal levels must have occurred during the strike-slip event because very shallow level faulting also overprints the metamorphic basement, and rhyolite dykes cut these structures. This indicates considerable exhumation during the transpressive event and also even more considerable lateral offset along the strike-slip faults.

The ^{40}Ar–^{39}Ar laser ablation ages place the waning stages of semi-ductile strike-slip shearing into the Mid Jurassic at 174–165 Ma. This is compatible with the age of 160.5 ± 1.7 Ma from sample CH02-78 from one of the rhyolite dykes cross-cutting the shear zones. The age of 160.5 ± 1.7 Ma indicates that most of the metamorphic basement has reached uppermost crustal levels by this time. The poorly defined crystallization age of 132 Ma of sample CH02-77 from a dyke with striated fault planes (Fig. 5c) shows that brittle faulting associated with strike-slip deformation also occurred in Early Cretaceous time. The resetting event at 119 Ma detected in sample CH02-77 could have been caused by this deformation, because there is no intrusive activity known in the region at that time. This vague age constraint and the structural relationships in the Middle Triassic Punta Tomás Breccia show that strike-slip shearing was apparently a long-lived event spanning more than 50 Ma from at least Mid Jurassic to Early Cretaceous times.

The outcrop of the Arrayán Formation might represent a transpressional syncline. Since shear zone 1 in Figure 2 is cut by a 161 Ma old rhyolite dyke, the age of this syncline would have to be older than 161 Ma and probably originated during semi-ductile sinistral transpression in Jurassic time.

The ZFT ages reported by Willner *et al*. (2011) indicate cooling below 280 ± 30 °C of block X in Figure 2 after about 100 Ma. Depending on the thermal structure of the crust, 280 ± 30 °C translates to depths of ~10–15 km. Because the block with the ~100 Ma ZFT ages is adjacent to blocks with ZFT ages > ~250 Ma and the cooling of block X below 280 ± 30 °C took place about 70 Ma after synkinematic recrystallization of white mica in the Punta Tomás shear zone, the juxtaposition of the blocks probably occurred after Mid Cretaceous time by brittle deformation.

We discuss several options: (1) The most simple and also most speculative option is to assume that the small area with the three ~100 Ma ZFT ages SW of Punta Tomás is underlain by a Mid Cretaceous pluton that caused resetting of the ZFT ages in the contact aureole. A similar case has been reported from south Chile by Thomson & Hervé (2002) who also found much younger Cretaceous ZFT ages in the accretionary complex rocks.

(2) Shear zone 1 in Figure 2 acted as a major top-to-the-W displacing thrust during Mid Cretaceous shortening (Arancibia, 2004). Erosional exhumation in the hangingwall of the thrust caused cooling of zircon in block X below 280 ± 30 °C. However, to explain the 274 ± 18 Ma ZFT age east of shear zone 2 (Fig. 2), one would need to envisage a top-to-the-E normal fault reactivation of shear zone 2. There is no structural evidence for coeval top-to-the-W thrusting and top-to-the-E normal faulting, and therefore we consider this option unlikely.

(3) Sinistral strike-slip shear zones could have been reactivated at ~100 Ma. Both shear zones 1 and 2 in Figure 2 would need to have been reactivated at this time to explain the young ZFT ages of block X. The western strand of shear zone 1 was not reactivated at this time because the cross-cutting rhyolite dyke dated at 161 Ma is not displaced. Because the average plunge of the stretching lineations is 15° (Fig. 3d) a relatively great net lateral displacement is needed for sliding in block X laterally and exhuming it at the same time. If, as argued above, the tectonic transport direction

https://doi.org/10.1017/S0016756811000653 Published online by Cambridge University Press

was steeper than the stretching lineations, the lateral displacement would have been smaller.

There is not much evidence for relatively great lateral transport (of, say, >10 km or so) in Mid Cretaceous time at Bahia Agua Dulce. In contrast, option (1) depends on a pluton in the subsurface for which there is no evidence. Overall, we envisage that options (1) and (3), or actually a combination of those two options, represent a possible scenario for explaining the ~100 Ma ZFT ages in block X.

6.b. Regional context

The age of 174–165 Ma for the end of semi-ductile sinistral transpressive shearing at 31–32° S shows that sinistral transpressional deformation of Jurassic age extends further south than hitherto envisaged. Recently, Willner, Richter & Ring (2009) reported structures resulting from sinistral transpressive deformation even from the Pichilemu/Constitución area at 34–35° S. However, Willner, Richter & Ring (2009) could not exactly bracket the timing of sinistral transpression, but also envisaged it to be Jurassic in age. Whether or not all of this transpressional deformation belongs to the Atacama Fault System is probably a semantic issue.

The evolution of the Atacama Fault System within the Jurassic–Early Cretaceous magmatic arc in the type region at 21–26° S was described by Scheuber & Gonzalez (1999). These authors argued that deformation was strongly partitioned into the magmatic arc during oblique subduction from 194 to 120 Ma. According to Scheuber & Gonzalez (1999), deformation was strictly bound to the magmatic arc and resulted in four stages of changing contractional and extensional regimes depending on the degree of coupling between the upper and lower plate. During stage I (194–155 Ma), sinistral arc-parallel strike-slip occurred in deep to shallow crustal levels of the arc including deformed plutons of the granulite to amphibolite-facies Bolfin Complex and two sets of conjugate greenschist-facies shear zones. Strike-slip shearing and thrusting in a NW–SE direction is interpreted to be the result of strong coupling between the downgoing and the overriding plate. Slab rollback and plate decoupling is supposed to have caused arc-normal extension with ductile to brittle normal faults between 160–150 Ma (stage II). During stage III (155–147 Ma), two bimodal dyke systems developed during two reversals of strike-slip deformation to a dextral sense and back to a sinistral shear sense. The last phase of sinistral strike-slip faulting was associated with brittle contractional structures. This transpressional event was again interpreted to be the result of strong plate coupling until 125 Ma (stage IV). After 120 Ma deformation moved continuously eastward with the magmatic arc.

If we compare our results with nearby areas and with the evolution in the type area of the Atacama Fault System, some correlations become evident. The derived ^{40}Ar–^{39}Ar ages of the two rhyolite dykes at 161 Ma and 132 Ma concur with a similar ^{40}Ar–^{39}Ar age of 138 Ma of K-feldspar from a rhyolite dyke at 34° S (Willner *et al*. 2005) and not well-defined ages of 213–133 Ma for mafic dykes at 31–32° S (Irwin *et al*. 1988; K–Ar dating of hornblende). The ages are close to the time of an envisaged short period of arc-normal extensional deformation at the Atacama Fault System (~160–150 Ma) at 21–26° S that was accompanied and followed by the intrusion of two generations of dykes, the first generation of which strikes NE and the younger one strikes NW (Scheuber & Gonzalez, 1999).

At 31–32° S we found no evidence for arc-normal extension. The 161–132 Ma old dykes postdate the intense semi-ductile transpressional deformation in our study area. The 132 Ma old dyke shows that shallow-level sinistral transpression continued in Early Cretaceous time. Despite the fact that we found no evidence for any interval of extensional deformation, the kinematic results of the prominent semi-ductile sinistral shear zones, their position within metamorphic basement inliers in the Jurassic–Early Cretaceous magmatic arc and the ^{40}Ar–^{39}Ar spot ages of 174–165 Ma coincide with the main stage of sinistral strike-slip deformation of the Atacama Fault System at 194–155 Ma (Scheuber & Gonzalez, 1999). However, at 31–32° S this deformation event occurred at higher crustal levels than further north.

We tentatively concur with Scheuber & Gonzalez (1999) that the sinistral transpressive structures probably resulted from NW-directed Jurassic–Early Cretaceous plate convergence and suggest a high degree of coupling between the downgoing and the overriding plates. Sinistral transpression apparently strongly affected inliers of the Chilean late Palaeozoic accretionary belt within the Jurassic–Early Cretaceous magmatic arc.

There is a possibility that at least two of the strike-slip shear zones were reactivated at ~100 Ma during a shortening event in the Mid Cretaceous magmatic arc. Arancibia (2004) showed that the contractional Silla del Gobernador shear zone developed at 32° S in the Cretaceous magmatic arc. The presently exposed section of the Silla del Gobernador shear zone formed under greenschist-facies metamorphism and was subsequently severely deformed in the brittle crust. The Silla del Gobernador shear zone resulted from WNW/W-oriented lithospheric shortening. This shortening direction is similar to the shortening direction reported herein for the earlier sinistral transpression deformation. Therefore, it is likely that at least some of the NNW-striking shear zone was sinistrally reactivated during this Mid Cretaceous shortening event.

7. Conclusions

We described structures resulting from transpressive sinistral strike-slip faulting in metamorphic basement rocks near Bahia Agua Dulce at 31–32° S in north-central Chile. The most conspicuous structures are

https://doi.org/10.1017/S0016756811000653 Published online by Cambridge University Press

sub-vertical semi-ductile NNW-striking strike-slip shear zones in which chlorite and sericite grew and white mica and quartz recrystallized dynamically. Sinistral strike-slip faulting was accompanied by the development of largely upright folds at the 10–100 metre scale. The folds have axes sub-parallel to the strike-slip shear zones and indicate a component of shortening parallel to the shear-zone boundaries. ^{40}Ar–^{39}Ar laser ablation ages of synkinematically recrystallized white mica in the shear zones provide an age of 174–165 Ma for the waning stage of semi-ductile sinistral shearing. However, a 132 Ma old rhyolitic dyke has been affected by brittle faulting. Fault-slip analysis shows that the kinematics of the faulting event is similar to the one of the semi-ductile shearing event, suggesting that sinistral transpression was a prolonged event that continued during exhumation until after 132 Ma. Our data show that sinistral transpression affected not only the major part of the Jurassic–Early Cretaceous magmatic arc, but also inliers of the late Palaeozoic accretionary complex within this prominent arc.

We have correlated sinistral transpression with the regional Atacama Fault System hitherto only known from north Chile. If this correlation was accepted then the absence of any Late Jurassic extension at 31–32° S may indicated N–S variations in the degree of plate coupling along the palaeo-Andean margin. The correlation highlights that sinistral strike-slip deformation affected a huge part of the Jurassic and Early Cretaceous fore-arc in Chile. It furthermore suggests a high degree of plate coupling along the palaeo-Andean margin during that time at 31–32° S.

Acknowledgements. Funded by Deutsche Forschungsgemeinschaft (Ri538/21; Ma1160/24) and the German–Chilean BMBF–CONICYT co-operation project (Chl 01A 6A). We thank Werner von Gosen and Johannes Glodny for constructive reviews and Mark Allen for editorial handling. S. Rebolledo introduced us to the study area and R. Charrier contributed with numerous discussions.

References

AGUIRRE, L., HERVÉ, F. & GODOY, E. 1972. Distribution of metamorphic facies in Chile: an outline. *Krystallinikum* **9**, 7–19.

ARANCIBIA, G. 2004. Mid-Cretaceous crustal shortening: evidence from a regional-scale ductile shear zone in the Coastal Range of central Chile (32° S). *Journal of South American Earth Sciences* **17**, 209–26.

BOLHAR, R. & RING, U. 2001. Deformation history of the Yolla Bolly terrane at Leech Lake Mountain, Eastern Belt, Franciscan Subduction Complex, Californian Coast Ranges. *Geological Society of America Bulletin* **181**, 181–95.

BRANDON, M. T. & VANCE, J. A. 1992. Tectonic evolution of the Cenozoic Olympic subduction complex, Washington State, as deduced from fission track ages for detrital zircons. *American Journal of Science* **292**, 565–636.

CHARRIER, R., PINTO, L. & RODRÍGUEZ, M. P. 2008. Chapter 3 Tectonostratigraphic evolution of the Andean orogen in Chile. In *The Geology of Chile* (eds T. Moreno & W. Gibbons), pp. 21–114. London: The Geological Society.

CECIONI, G. & WESTERMANN, G. 1968. The Triassic/Jurassic marine transition of coastal central Chile. *Pacific Geology* **1**, 41–75.

FEEHAN, J. G. & BRANDON, M. T. 1999. Contribution of ductile flow to exhumation of low-temperature, high-pressure metamorphic rocks: San Juan-Cascade nappes, NW Washington State. *Journal of Geophysical Research B: Solid Earth* **104**, 10883–902.

GLODNY, J., LOHRMANN, J., ECHTLER, H., GRÄFE, K., SEIFERT, W., COLLAO, S. & FIGUEROA, O. 2005. Internal dynamics of a paleoaccretionary wedge: insights from combined isotope tectonochronology and sandbox modelling of the south-central Chilean forearc. *Earth and Planetary Science Letters* **231**, 23–39.

GLODNY, J., RING, U. & KÜHN, A. 2008. Coeval high-pressure metamorphism, thrusting, strike-slip and extensional shearing in the Tauern Window, Eastern Alps. *Tectonics* **27**, TC4004, doi:10.1029/2007TC002193, 27 pp.

GROCOTT, J., BROWN, M., DALLMEYER, R. D., TAYLOR, G. K. & TRELOAR, P. J. 1994. Mechanisms of continental growth in extensional arcs: an example from the Andean plate-boundary zone. *Geology* **22**, 391–4.

GROCOTT, J. & TAYLOR, G. K. 2002. Magmatic arc fault systems, deformation partitioning and emplacement of granitic complexes in the Coastal Cordillera, north Chilean Andes (25°30′S to 27°00′S). *Journal of the Geological Society, London* **159**, 425–42.

HERVÉ, F. 1988. Late Paleozoic subduction and accretion in Southern Chile. *Episodes* **11**, 183–8.

HERVÉ, F., FAÚNDEZ, V., CALDERÓN, M., MASSONNE, H.-J. & WILLNER, A. P. 2007. Metamorphic and plutonic basement complexes. In *The Geology of Chile* (eds T. Moreno & W. Gibbons), pp. 5–19. London: The Geological Society.

IRWIN, J. J., GARCÍA, C., HERVÉ, F. & BROOK, M. 1988. Geology of part of a long-lived dynamic plate margin: the coastal cordillera of north-central Chile, latitude 30°51′–31°–32° S. *Canadian Journal of Earth Sciences* **25**, 603–24.

LANPHERE, M. A. & DALRYMPLE, G. B. 2000. First-principles calibration of ^{38}Ar tracers: implications for the ages of $^{40}Ar/^{39}Ar$ fluence monitors. *US Geological Survey Professional Paper* **1621**, 10 pp.

LAYER, P. W. 2000. Argon-40/Argon-39 age of the El'gygytgyn impact event, Chukotka, Russia. *Meteoritics and Planetary Science* **35**, 591–9.

LAYER, P. W., HALL, C. M. & YORK, D. 1987. The derivation of $^{40}Ar/^{39}Ar$ age spectra of single grains of hornblende and biotite by laser step heating. *Geophysical Research Letters* **14**, 757–60.

MARRETT, R. & ALLMENDINGER, R. W. 1990. Kinematic analysis of fault-slip data. *Journal of Structural Geology* **15**, 973–86.

MCDOUGALL, I. & HARRISON, T. M. 1999. *Geochronology and Thermochronology by the $^{40}Ar/^{39}Ar$-Method*. Oxford: Oxford University Press, 269 pp.

PARADA, M. A., LOPEZ-ESCOBAR, L., OLIVEROS, V., FUENTES, F., MORATA, D., CALDERÓN, M., AGUIRRE, L., FÉRAUD, G., ESPINOZA, F., MORENO, H., FIGUEROA, O., MUNOZ BRAVO, J., TRONCOSO VÁSQUEZ, R. & STERN, C. R. 2008. Chapter 4 Andean magmatism. In *The Geology of Chile* (eds T. Moreno & W. Gibbons), pp. 115–46. London: The Geological Society.

REBELLEDO, S. & CHARRIER, R. 1994. Evolución del basamento Paleozoico en el área de Punta Claditas, Región de Coquimbo, Chile (31–32° S). *Revista Geológica de Chile* **21**, 55–69.

REBELLEDO, S., SOLARI, M. & CONTRERAS, J. P. 2003. Foliaciones S-C en rocas Paleozoicas y Triásicas del sector de Puerto Manso, IV Región de Coquimbo. Actas 10. Congreso Geológico Chileno 2003, 1–6.

RIVANO, S. & SEPÚLVEDA, P. 1983. Hallazgo de foraminíferos del Carbonífero Superior en la Formación Huentelauquén. *Revista Geológica de Chile* **19–20**, 25–35.

RIVANO, S. & SEPÚLVEDA, P. 1985. Las calizas de la Formación Huenteauquén: Depósitos de aguas templadas a frías en el Carbonífero Superior-Pérmico Inferior. *Revista Geológica de Chile* **25–26**, 29–38.

RICHTER, P., RING, U., WILLNER, A. P. & LEISS, B. 2007. Structural contacts in subduction complexes and their tectonic significance: the late Palaeozoic coastal accretionary wedge of central Chile. *Journal of the Geological Society, London* **164**, 203–14.

RING, U. 2008. The tectonic evolution of the Franciscan Subduction Complex: implications for the exhumation of high-pressure rocks in subduction-related accretionary wedges. *Geological Society of America Special Paper* **445**, 1–91.

RING, U. & BRANDON, M. T. 1994. Kinematic data for the Coast Range fault and implications for exhumation of the Franciscan complex. *Geology* **22**, 735–8.

RING, U. & BRANDON, M. T. 1999. Ductile strain, coaxial deformation and mass loss in the Franciscan complex: implications for exhumation processes in subduction zones. In *Exhumation Processes: Normal faulting, ductile flow and erosion* (eds U. Ring, M. T. Brandon, G. S. Lister & S. Willett), pp. 55–85. Geological Society of London, Special Publication no. 154.

RING, U. & BRANDON, M. T. 2008. Exhumation settings. Part I: relatively simple cases. *International Geological Review* **50**, 97–120.

RING, U., BRANDON, M. T. & RAMTHUN, A. 2001. Solution-mass-transfer deformation adjacent to the Glarus thrust, with implications for the tectonic evolution of the Alpine wedge in eastern Switzerland. *Journal of Structural Geology* **23**, 1491–505.

ROBIN, P.-Y. F. & CRUDEN, A. R. 1994. Strain and vorticity patterns in ideally ductile transpression zones. *Journal of Structural Geology* **16**, 447–66.

SAMSON, S. D. & ALEXANDER, E. C. 1987. Calibration of the interlaboratory $^{40}Ar/^{39}Ar$ dating standard, MMhb1. *Chemical Geology* **66**, 27–34.

SCHEUBER, E. & ANDRIESSEN, P. M. 1990. The kinematic significance of the Atacama Fault zone, northern, Chile. *Journal of Structural Geology* **21**, 243–57.

SCHEUBER, E. & GONZALEZ, G. 1999. Tectonics of the Jurassic-Early Cretaceous magmatic arc of the north Chilean Coastal Cordillera (22°–26° S): a story of crustal deformation along a convergent plate boundary. *Tectonics* **18**, 895–910.

STEIGER, R. H. & JÄGER, E. 1977. Subcommission on geochronology: convention on the use of decay constants in geo and cosmochronology. *Earth and Planetary Science Letters* **36**, 359–62.

THIELE, R. & HERVÉ, F. 1984 Sedimentación y tectónica de antearco en los terrenos preandinos del Norte Chico, Chile. *Revista Geológica de Chile* **22**, 61–75.

THOMSON, S. N. & HERVÉ, F. 2002. New time constraints for metamorphism at the ancestral Pacific Gondwana margin of southern Chile (42° S–52° S). *Revista Geológica de Chile* **29**, 255–71.

WILLNER, A. P., GERDES, A. & MASSONNE, H.-J. 2008. History of crustal growth and recycling at the Pacific convergent margin of South America at latitudes 29°–36° S revealed by a U-Pb and Lu-Hf isotope study of detrital zircon from late Paleozoic accretionary systems. *Chemical Geology* **253**, 114–29.

WILLNER, A. P., MASSONE, H.-J., RING, U., SUDO, M. & THOMSON, S. N. 2011. *P–T* evolution and timing of a late Palaeozoic fore-arc system and its heterogeneous Mesozoic overprint in north-central Chile (latitudes 31–32° S). *Geological Magazine* **149**, 177–207.

WILLNER, A. P., RICHTER, P. & RING, U. 2009. Structural overprint of a late Paleozoic accretionary system in north-central Chile (34°–35° S) during postaccretional deformation. *Andean Geology* **36**, 17–36.

WILLNER, A. P., THOMSON, S. N., KRÖNER, A., WARTHO, J. A., WIJBRANS, J. & HERVÉ, F. 2005. Time markers for the evolution and exhumation history of a late Palaeozoic paired metamorphic belt in central Chile (34°–35°30′ S). *Journal of Petrology* **46**, 1835–58.

YORK, D., HALL, C. M., YANASE, Y., HANES, J. A. & KENYON, W. J. 1981. 40Ar/39Ar dating of terrestrial minerals with a continuous laser. *Geophysical Research Letters* **8**, 1136–8.